Brain Research Bulletin 211 (2024) 110949

Contents lists available at ScienceDirect

Brain Research Bulletin

journal homepage: www.elsevier.com/locate/brainresbull

Research report

Abnormal functional connectivity of white-matter networks and gray-white matter functional networks in patients with NMOSD

Xincui Wan [a,1], Yingjie Tang [b,1], Yu Wu [c], Zhenming Xu [a], Wangsheng Chen [a], Feng Chen [a], Cheng Luo [b,*], Fei Wang [a,**]

[a] Department of Radiology, Hainan General Hospital, Hainan Affiliated Hospital of Hainan Medical University, Haikou 570311, China
[b] The Clinical Hospital of Chengdu Brain Science Institute, MOE Key Lab for Neuroinformation, Center for Information in Medicine, School of Life Science and Technology, University of Electronic Science and Technology of China, Chengdu 610054, China
[c] Department of Neurology, Hainan General Hospital, Hainan Affiliated Hospital of Hainan Medical University, Haikou 570311, China

ARTICLE INFO

Keywords:
Neuromyelitis optica spectrum disorder
Functional connectivity
Functional covariance connectivity
Resting-state fMRI

ABSTRACT

Cognitive impairment (CI) has been reported in 29–70% of patients with neuromyelitis optica spectrum disorder (NMOSD). Abnormal white matter (WM) functional networks that correlate with cognitive functions have not been studied well in patients with NMOSD. The aim of the current study was to investigate functional connectivity (FC), spontaneous activity, and functional covariance connectivity (FCC) abnormalities of WM functional networks in patients with NMOSD and their correlation with cognitive performance. Twenty-four patients with NMOSD and 24 healthy controls (HCs) were included in the study. Participants underwent brain resting-state functional magnetic resonance imaging (fMRI) and the Montreal Cognitive Assessment (MoCA). Eight WM networks and nine gray matter (GM) networks were created. In patients, WM networks, including WM1–4, WM1–8, WM2–6, WM2–7, WM2–8, WM4–8, WM5–8 showed reduced FC ($P < 0.05$). All WM networks except WM1 showed decreased spontaneous activity ($P < 0.05$). The major GM networks demonstrated increased/decreased FC ($P < 0.05$), whereas GM7-WM7, GM8-WM4, GM8-WM6 and GM8-WM8 displayed decreased FC ($P < 0.05$). The MoCA results showed that two-thirds (16/24) of the patients had CI. FC and FCC in WM networks were correlated negatively with the MoCA scores ($P < 0.05$). WM functional networks are multi-layered. Abnormal FC of WM functional networks and GM functional networks may be responsible for CI.

Clinical relevance statement

This study adds to the evidence supporting the presence of multi-layered WM functional networks and extends the abnormalities of WM dysfunction in patients with NMOSD.

Key points

- WM functional networks in patients with NMOSD showed reduced FC and decreased spontaneous activity.
- The major GM functional networks in patients with NMOSD demonstrated increased/decreased FC.

1. Introduction

Neuromyelitis optica spectrum disorder (NMOSD) is an inflammatory disease with antibodies against the aquaporin-4 (AQP4) water channel, manifested by optic neuritis, longitudinally extensive transversal myelitis, and/or diencephalic symptoms. Cognitive impairment (CI) has been reported in 29–70% of patients with NMOSD (Moore et al., 2016, Salama et al., 2020, Meng et al., 2017, Vanotti et al., 2013, Kim et al., 2016, Blanc et al., 2008, Chanson et al., 2011, He et al., 2011, Hollinger et al., 2016, Kawahara et al., 2014, Kim et al., 2016, Zhang et al., 2015). In NMOSD, there remains a disagreement between imaging findings and CI. NMOSD brain lesions, including typical lesions in

* Correspondence to: The Clinical Hospital of Chengdu Brain Science Institute, MOE Key Lab for Neuroinformation, Center for Information in Medicine, School of Life Science and Technology, University of Electronic Science and Technology of China, Second North Jianshe Road, Chengdu 610054, China.
** Correspondence to: Department of Radiology, Hainan General Hospital, Hainan Affiliated Hospital of Hainan Medical University, 19 Xiu-hua St , Haikou 570311, China.
E-mail addresses: chengluo@uestc.edu.cn (C. Luo), 15103693890@163.com (F. Wang).
[1] Co-first authors.

https://doi.org/10.1016/j.brainresbull.2024.110949
Received 20 January 2024; Received in revised form 10 March 2024; Accepted 11 April 2024
Available online 12 April 2024

Table 1
Demographic information of the subjects.

	NMOSD Mean (SD)	HC Mean (SD)	p value[a]
Sex (male/female)	1/23	1/23	-
Age (years)	40.46 (14.36)	40.38 (12.68)	0.983
Education (years)	6.2 (3.9)	6.7 (3.5)	0.65
EDSS	3.60 (1.62)	-	-
MoCA	22.92 (5.43)	27.12 (1.30)	0.001*

[a] P values were obtained from the two-sample *t*-test.
* $P < 0.05$

AQP4-rich regions, multiple sclerosis (MS)-like lesions that do not meet MS criteria, and nonspecific lesions were shown on brain MRI (Wang et al., 2011). However, focal brain lesions in NMOSD and CI have been reported to have no statistical association, different from those with multiple sclerosis (Liu et al., 2015, Kim et al., 2017). Reduced global and/or focal white matter (WM) volumes, including the brainstem, corticospinal tracts, corpus callosum, superior longitudinal fascicle, and inferior longitudinal fascicle, were responsible for CI (Blanc et al.,2012, Finke et al.,2016). Hyun et al. reported a significant link between reduced volume of the thalamus or hippocampus and CI in patients with NMOSD, which contrasted with the absence of gray matter (GM) atrophy (Hyun et al.,2017). The WM networks revealed two disturbed sub-networks and a decreased overall strength of brain networks in diffusion tensor imaging (DTI) studies utilizing the graph theory (Cho et al.,2018, Zheng et al.,2021). Liu et al. reported that changes in the small-world topology of WM structural networks, such as the precuneus, a hub in the default mode network, may cause CI in patients (Liu et al., 2012). Although DTI research described the anatomical makeup of the WM, it was unable to identify neuronal activity or functions. In resting-state functional MRI (fMRI), patients showed reduced baseline brain activity in cognition-related brain regions, such as the lingual gyrus, precuneus, and posterior cingulate cortex (Liu et al.,2011). To complete a modified version of paced auditory serial addition tasks, the cerebellum, left insula, right cingulate gyrus, right inferior parietal gyrus, and both bilateral superior temporal gyri were engaged in patients with NMOSD (Wang et al.,2017).

Recent resting-state fMRI investigations have shown that functional brain activity is present in WM(Power et al.,2011, Shirer et al.,2012, Peer et al.,2017). Dysfunctional WM networks play a role in the onset of schizophrenia or epilepsy (Cui et al.,2021, Jiang et al.,2019). A recent study using resting-state fMRI and graph theory reported a correlation between Expanded Disability Status Scale (EDSS) scores and the visual/sensorimotor network reorganization in NMOSD (Bigaut et al., 2019). To the best of our knowledge, there have been few reports on WM network correlates of cognitive functions in patients with NMOSD. We hypothesized that WM networks are disturbed in patients with NMOSD, and these alterations may be responsible for CI.

2. Materials and methods

2.1. Participants

The retrospective study was approved by the Hospital's institutional review board, and each participant provided written informed consent before taking part in the study.

Twenty-four patients with NMOSD and 24 age-, sex-, and education-matched right-handed HC were included. Patients aged from 20 to 50 years were recruited from the Department of Neurology in our hospital between January 01, 2018 and December 31, 2022. The inclusion criteria were: (1) conventional brain and/or spinal cord imaging findings that were consistent with the diagnostic criteria of NMOSD (Wingerchuk et al., 2015); (2) being in a remission period (at least 4 weeks apart from acute relapses and intravenous steroid administration); and (3) being AQP4 antibody positive (in a cell-based assay). The exclusion criteria were: (1) history of an injury or other clinical neurologic diseases; and (2) image artifacts or incomplete clinical information. All participants underwent a resting-state fMRI of the brain and the Montreal cognitive assessment (MoCA). MoCA was used for the rapid screening of cognitive function abnormalities. The demographic information of the subjects is shown in Table 1.

2.2. Image acquisition

Imaging data were collected using a 3.0-Tesla MRI scanner (Siemens Healthcare, Erlangen, Germany) with a 32-channel whole head coil. High-resolution T1 weighted images (T1WIs) were obtained by using a three-dimensional fast spoiled gradient-echo sequence. The scanning parameters included: repetition time (TR) = 2530 ms; echo time (TE) = 2.98 ms; flip angle (FA) = 7°; field of view (FOV) = 25.6 cm× 25.6 cm; matrix size = 256 × 256; slice thickness = 1 mm (no gap); voxel size = 1.0 ×1.0 ×1.0 mm^3; and 192 slices. Resting-state functional data were obtained using a gradient-echo echo-planar imaging sequence. The main scanning parameters were as follows: TR = 2000 ms; TE = 30 ms; FA = 90; FOV = 22.4 cm× 22.4 cm; matrix size = 64 × 64; slice thickness = 3.5 mm (no gap); voxel size =3.50×3.50×3.50 mm^3; 32 slices; and scanning time = 480 s (240 volumes). Participants were instructed to close their eyes without falling asleep during scanning.

2.3. Data preprocessing

The SPM12 (www.fil.ion.ucl.ac.uk/spm) and DPABI (http://rfmri.org/dpabi) toolkits were used to preprocess the functional image and T1 image. The fMRI preprocessing steps were as follows: (a) removing the first five time points; (b) a slice-time correction; (c) a realignment and exclusion of all subjects with maximum head motion > 2° or 2 mm; (d) linear detrending; (e) regressing out the nuisance signal (including a 24-parameter motion correction and the mean cerebrospinal fluid (CSF) signals); (f) bandpass filtering (0.01–0.15 Hz); (g) spatial smoothing (FWHM = 4 mm) carried out individually within the WM or GM masks to prevent the mixing of WM and GM signals; WM, GM, and CSF were specifically segregated in native space from each individual T1 image. To identify WM or GM masks, the resulting T1 segmentation images were co-registered to the functional space for each participant (the threshold was set at 0.5). Within each of the two masks, the distinct functional pictures were smoothed (FWHM = 4 mm); and (h) normalization using the typical MNI template (Jiang et al.,2019).

2.4. Definition of a WM network

WM networks were defined using voxel-based functional connectivity (FC) (Jiang et al.,2019). The first step was to obtain a unified group-level WM mask based on high-resolution T1WIs. The details were as follows: For each subject, T1WIs were segmented into WM, GM, and CSF, and then normalized to the MNI template. For each voxel, it was identified as WM, GM, or CSF according to the maximum probability of the above segmentation results. This generated three masks of WM, GM, and CSF for each subject. The masks were then averaged across all subjects to obtain the percentage of subjects classified as WM. A percentage threshold of >60% was used to identify group-level WM masks. Finally, the group-level WM masks were co-registered with the functional space and resampled to the same voxel size as the fMRI images. This white matter network includes 17,716 voxels.

The second step applied the K-means clustering algorithm to obtain WM spatial networks. The specific details were as follows: In order to reduce the computational difficulty while retaining data features as much as possible, we used the exchange grid strategy to downsample the 17,716 voxels in the WM mask to 4426 nodes. The Pearson correlation coefficient was calculated between each voxel and each node in each subject's white matter mask, creating a 17,716 × 4426 correlation matrix. The correlation matrices of all subjects are averaged to obtain an

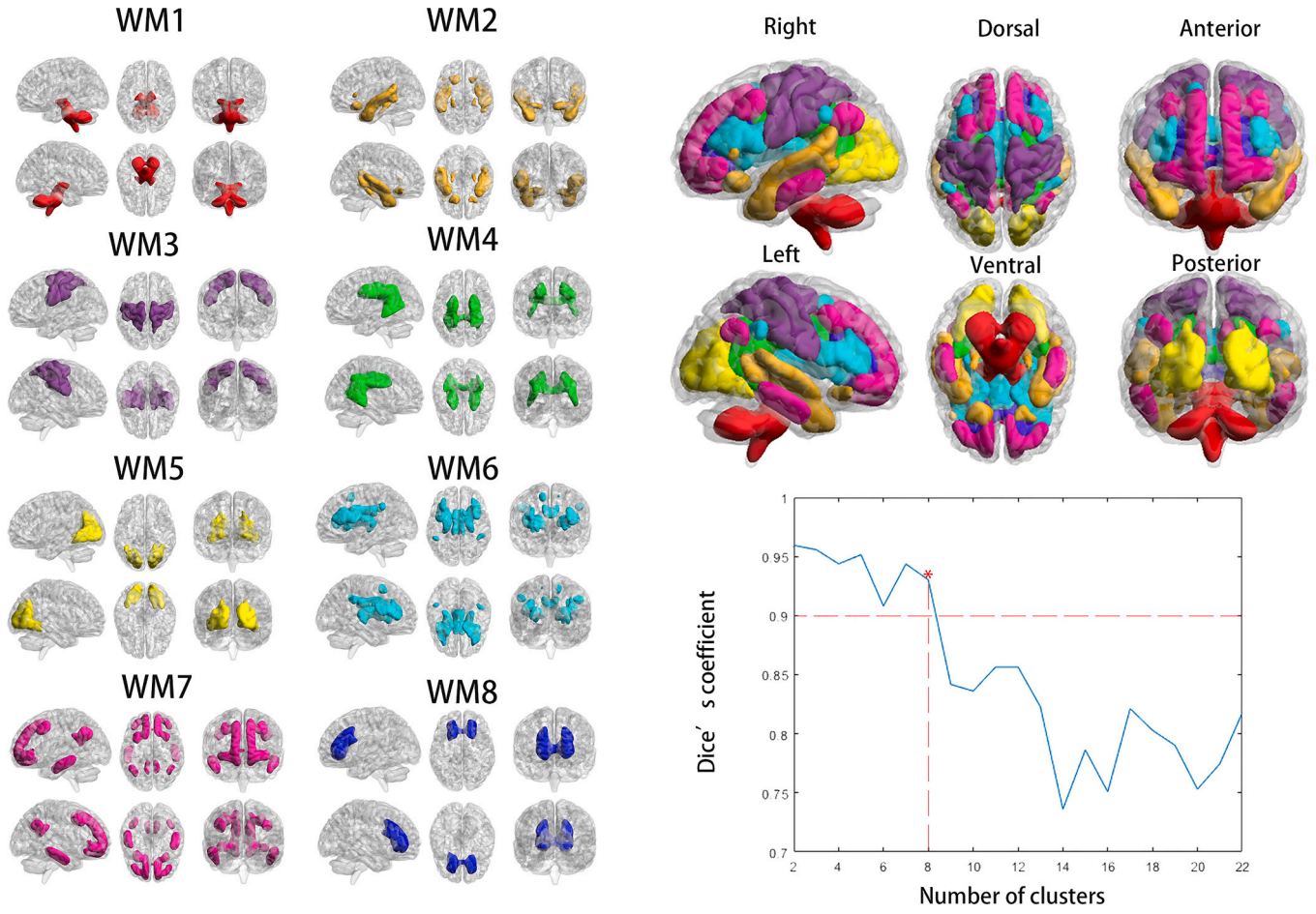

Fig. 1. White-matter functional networks and stability of clustering for different numbers of clusters, measured by Dice's coefficient.

Table 2
Distribution of WM networks.

Abbreviation	White-matter network	Layer
WM1	Cerebellum-brainstem network (CBN)	Superficial
WM2	Superior temporal network (STN)	Superficial
WM3	Precentral/postcentral network (PCN)	Superficial
WM4	Deep network (DN)	Deep
WM5	Occipital network (ON)	Superficial
WM6	Middle corpus callosum network (MCCN)	Middle
WM7	Frontotemporal network (FTN)	Superficial
WM8	Anterior corpus callosum network (aCCN)	Middle

average correlation matrix. Finally, a K-means clustering analysis (distance metric correlation, 10 replicates) was performed on the averaged correlation matrix.

The third step evaluated the stability of K (the number of clusters). The average connectivity matrix was randomly divided into four folds (17,716 × 1106), and adjacent matrices were calculated for each clustering result in each fold in order to measure the similarity of clustering results between any two folds. These adjacency matrices were then compared using the Dice coefficient, and the average Dice coefficient was used to assess cluster stability.

2.5. Spontaneous activity of WM functional networks

We performed a spectral analysis of the BOLD signal from each WM functional network using the Fourier transform and calculated the amplitude of oscillation at band A (0.01–0.15 Hz), band B (0.01–0.08 Hz), and band C (0.08–0.15 Hz). For each WM network, we calculated the average of the amplitudes in each frequency band to assess the degree of spontaneous activity of the WM mass. Finally, a two-sample *t*-test was used to compare the differences between patients with NMOSD and HCs.

2.6. FC/ functional covariance connectivity (FCC) of WM functional networks

To assess FC between different WM clusters, this study extracted the average of all voxel time series within each WM functional network as the time series of the WM functional network. The Pearson correlation coefficient of any two WM functional network time series was computed and converted into a Fisher z-score. In addition, to assess the relationship between WM functional network and GM functional network, this study also calculated Fisher's z-scores for the Pearson correlation coefficients between each WM functional network and each GM functional network. Since a large number of previous studies have obtained stable and reproducible GM functional networks(Power et al.,2011, Shirer et al.,2012, Peer et al.,2017), this study did not perform cluster analysis on GM functional networks, but used the GM functional network atlas obtained by the same calculation method in previous literature.

To estimate the covariant link between two WM functional networks based on their correlations with the entire GM, we used the FCC technique, which is based on the concept of "correlation of correlations." First, areas of GM (n = 96) were established using the Harvard-Oxford GM atlas. For GM voxels, the GM mask was employed as a limitation. Only the time series that fell within the intersection of the Harvard-Oxford atlas and the GM mask were retrieved. Second, a K*96 correlation matrix was created by calculating the Pearson's correlations

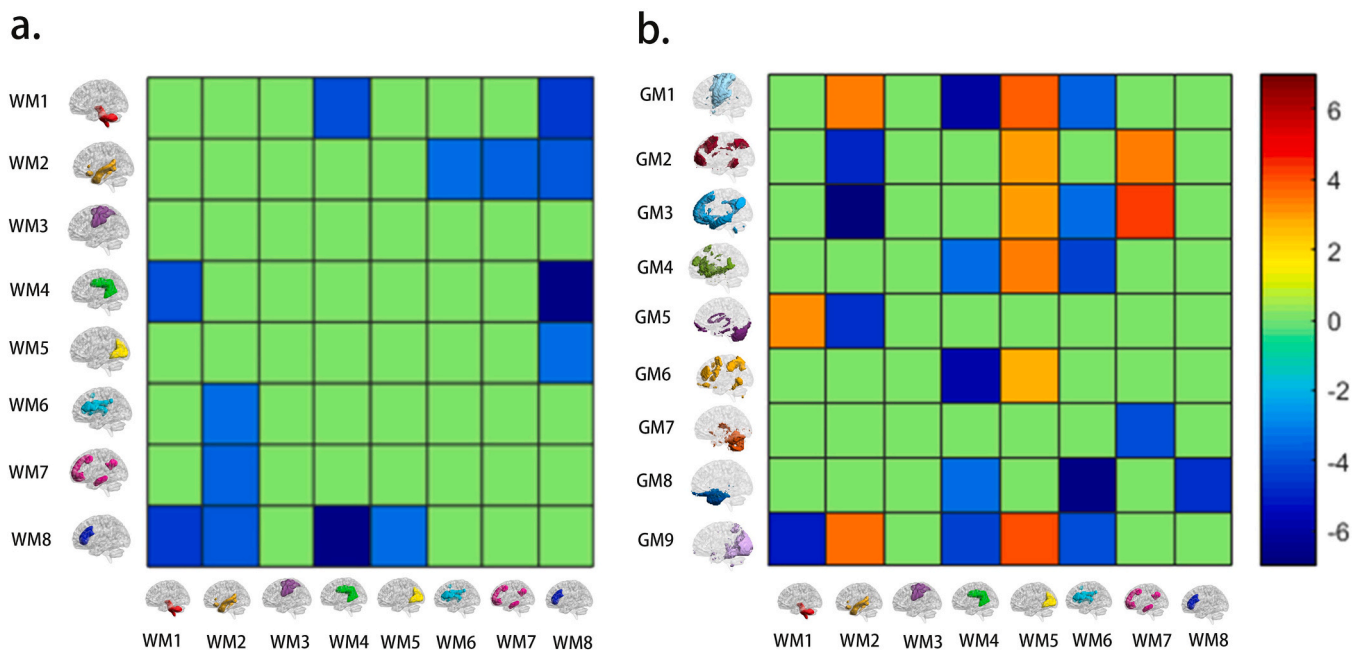

Fig. 2. Functional connectivity of the two WM networks (a) or the WM-GM networks (b). (P <0.05, FDR correction).

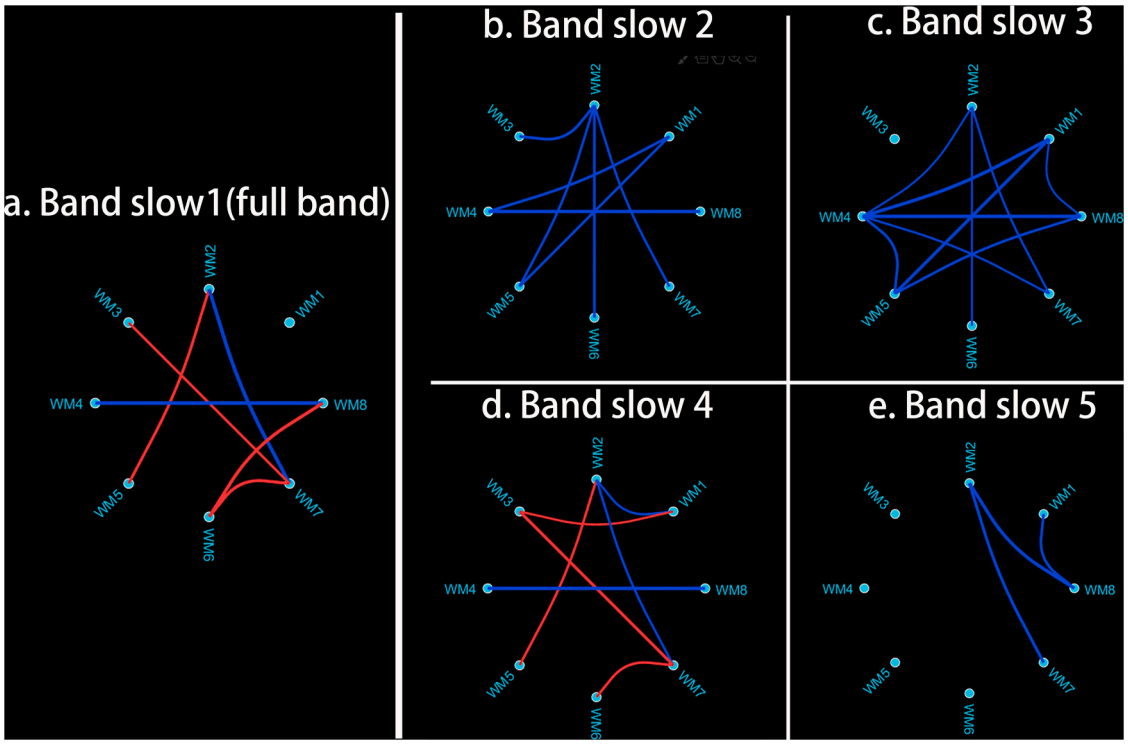

Fig. 3. Differences in functional covariance connectivity (FCC) between two groups in different bands. (a) Slow-1; (b) Slow-2; (c) Slow-3; (d) Slow-4; and (e) Slow-5. (p<0.05) The blue line represents reduced FCC of the NMOSD group relative to the HC group. The red line indicates increased FCC of the NMOSD group relative to the HC group.

between each WM network and each GM region (K is the number of WM networks). Third, a K*K FCC matrix was created by estimating the FCC between any two WM networks. The FCC_{ij} was defined as follows:

$$FCC_{ij}=corr(FC_i, FC_j)$$

where FC_i represents the vector of FC values between the WM network i and all 96 GM regions; FC_j represents the vector of FC values between the WM network j and all 96 GM regions; and FCC_{ij} represents the Pearson's correlation between FC_i and FC_j. In consideration of including time series from GM, bandpass filtering 0–0.25 Hz was applied according to the frequency feature of GM. Further, we changed the filtering band during preprocessing before calculating FCC in the whole brain mask, whereas every other step remained the same. Here, the low frequency range was separated into four bands in accordance with previously established criteria [25]: Slow-5 (0.01–0.027 Hz), Slow-4

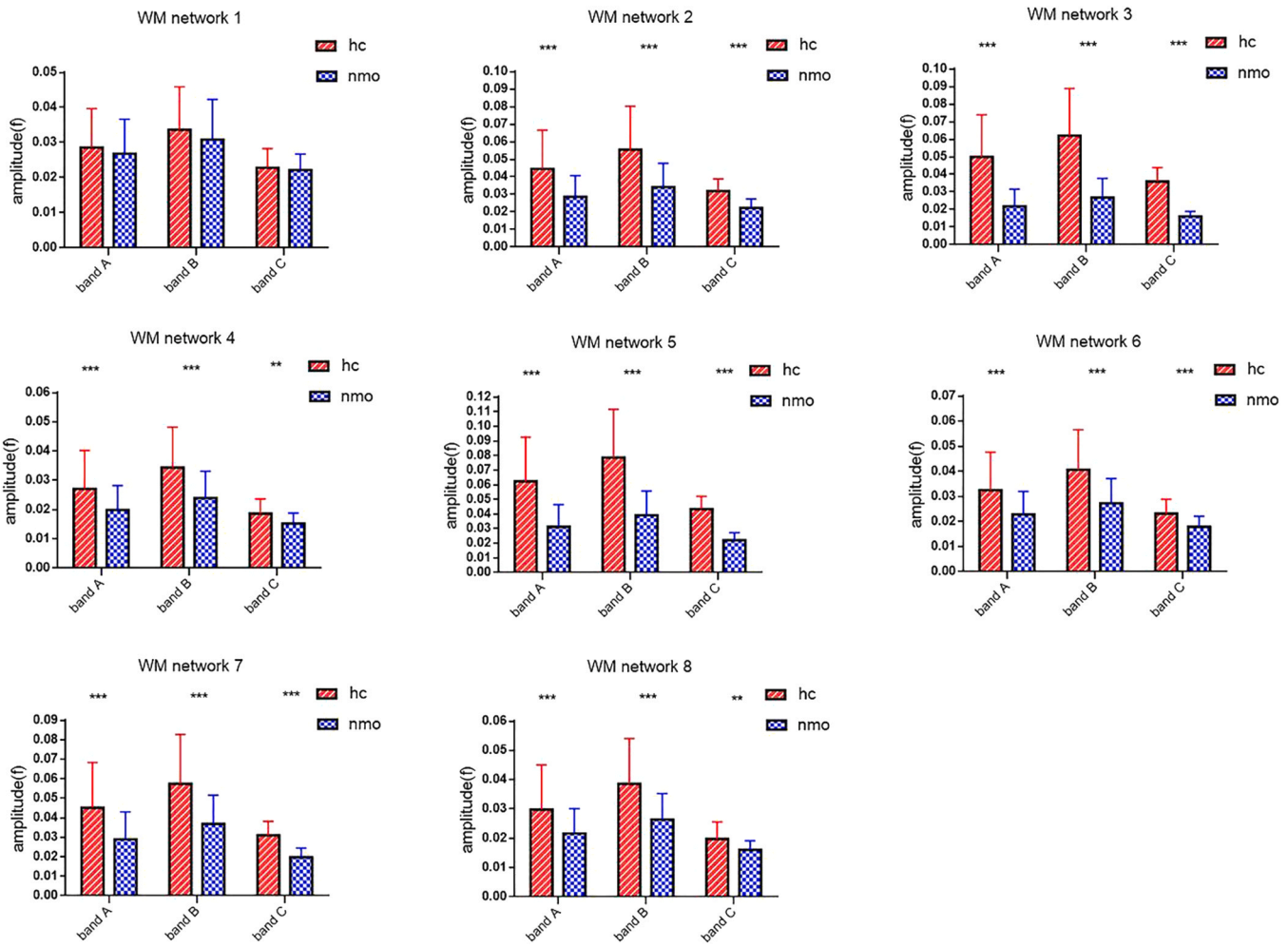

Fig. 4. Spontaneous activity of WM networks in patients with NMOSD and HCs at different frequency bands (Band A, Band B, and Band C). Two-sample *t*-test was used for statistical analysis. (*: P < 0.05, **: P < 0.01, ***: P < 0.001).

(0.027–0.073 Hz), Slow-3 (0.073–0.198 Hz), and Slow-2 (0.198–0.25 Hz). Slow-1 (0–0.25 Hz) was also investigated. FCC were computed for each participant and each frequency band in this study.

2.7. Statistical analysis

Two-sample *t*-tests were performed to identify significant differences in inter-network FC between the two groups. An FDR correction was used to correct for multiple comparisons. The FC and FCC values of the WM networks between the groups were extracted. Spearman's rank correlation was used to evaluate the relationship between FC, FCC, and MoCA scores. A result was considered statistically significant if the P value was less than 0.05.

3. Results

3.1. WM functional networks

In this study, we applied Dice's coefficient to assess the stability of the number of WM networks. K = 8 was discovered to be the most stable number (Dice's coefficient >0.90), and eight WM networks were created (Fig. 1). These networks are shown in Table 2 based on their spatial position[3].

3.2. FC/FCC in WM and GM-WM networks

Patients with NMOSD had decreased FC in all WM networks except WM3 (precentral/postcentral network, PCN) (Fig. 2.a).

The nine GM networks included GM1 (sensory-motor network, SMN), GM2 (frontal-parietal control network, FPCN), GM3 (default mode network, DMN), GM4 (ventral attention network, VAN), GM5 (posterior cerebellar network, pCN), GM6 (dorsal attention network, DAN), GM7 (anterior cerebellar network, aCN), GM8 (orbital frontal network, OFN), and GM9 (visual network, VN). The major GM-WM networks showed decreased FC and increased FC, but the cerebellar network (GM7) and the orbital frontal network (GM8) demonstrated decreased FC (Fig. 2.b).

The reduced FCC in WM2-WM7 was shared in Slow-1, Slow-2, Slow-3, Slow-4, and Slow-5, while the reduced FCC in WM4-WM8 was shared in Slow-1, Slow-2, Slow-3, and Slow-4 (Fig. 3).

3.3. Spontaneous activity of the WM networks

In different bands, All WM networks in the NMOSD group showed decreased spontaneous activity except WM1 (Fig. 4).

3.4. Correlation between FC, FCC, and MoCA scores

MoCA was used for the rapid screening of cognitive function impairment. It evaluates visuospatial/executive, naming, memory,

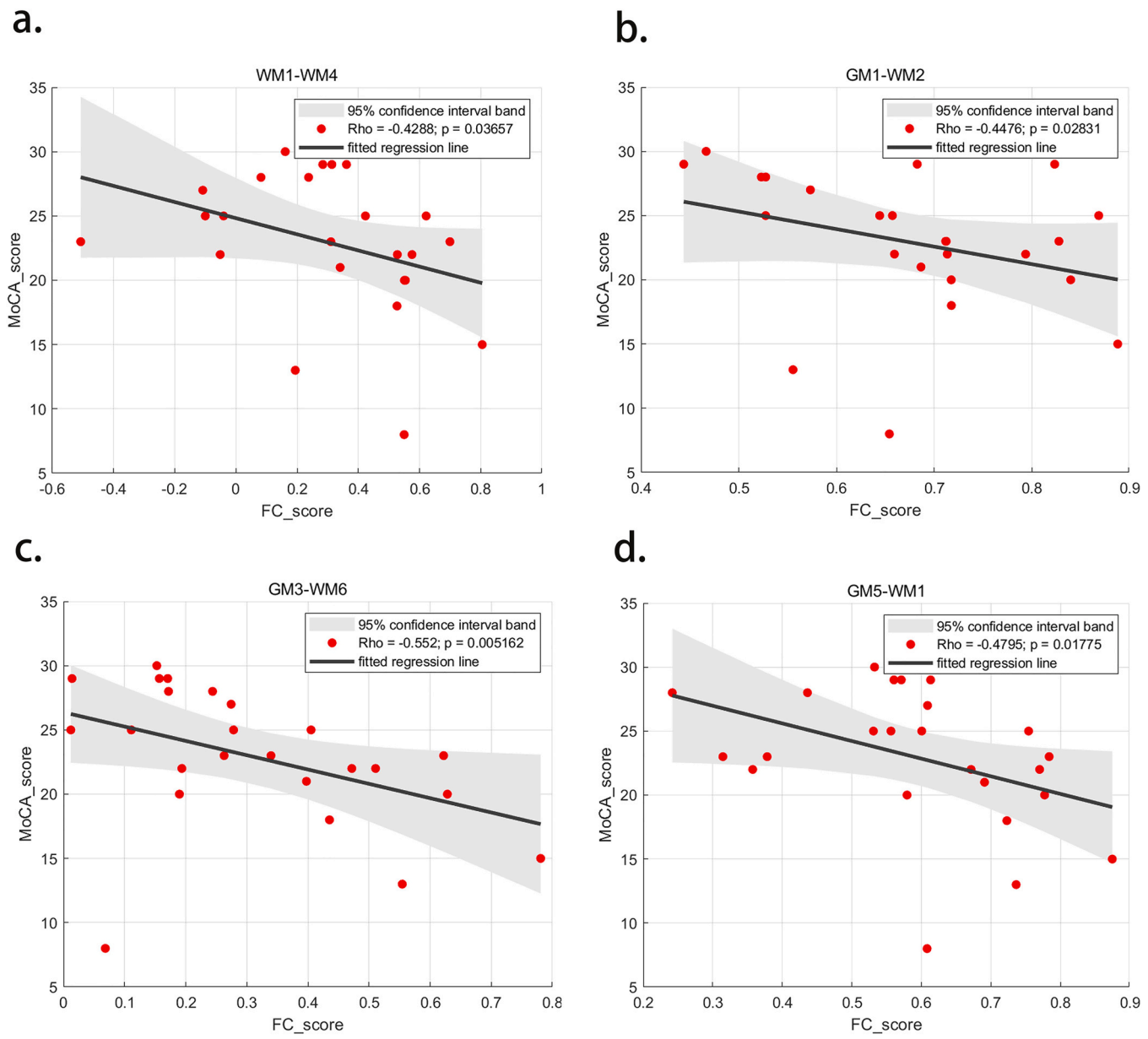

Fig. 5. A negative correlation between the MoCA scores and FC in different networks. (a). WM1-WM4. (b). GM1-WM2. (c). GM3-WM6. (d). GM5-WM1.

attention, language, abstraction, and orientation. The MoCA showed that two-thirds (16/24) of the patients had CI, of which 13 had mild impairment (between 18 and 26 points), 2 had moderate impairment (between 10 and 17 points), and 1 had severe impairment (less than 10).

In the NMOSD group, a negative correlation between the MoCA scores and FC was observed for WM1-WM4 (rho = −0.4288, p = 0.03657), GM1-WM2 (rho = −0.4476, p = 0.02831), GM3-WM6 (rho = −0.552, p = 0.005162), and GM5-WM1 (rho = −0.4795, p = 0.01775). These results are shown in Fig. 5.

Furthermore, a negative correlation was observed between the MoCA scores and FCC in WM6-WM7 (slow-1) (rho = −0.5538, p=0.004994), WM1-WM4 (slow-2) (rho = −0.4261, p=0.03786), WM2-WM7 (slow-2) (rho = −0.4851, p=0.01626), WM4-WM8 (slow-2) (rho = −0.5236, p=0.008642), WM4-WM8 (slow-3) (rho = −0.5822, p=0.002839), and WM1-WM3 (slow-4) (rho = −0.4476, p=0.02831) in the NMOSD group. These results are shown in Fig. 6.

4. Discussion

In resting-state fMRI, the functional connectivity of WM in patients with NMOSD is uncertain. In the present study, we first reported that (a) Multi-layered WM functional networks, reduced spontaneous activity, and decreased FC in WM networks were observed in patients with NMOSD. The low-frequency oscillation of the resting BOLD signal is a physiological indicator of spontaneous brain activity. (b) The major GM networks showed increased and decreased FC (including GM3, GM4, and GM6). (c) FC and FCC in WM networks were correlated negatively with the MoCA scores. These alterations may be responsible for CI.

Previous studies have reported that patients with NMOSD present with decreased functional connections and spontaneous activity in GM networks. Han et al. reported that the DMN, DAN, and thalamic networks had increased FC, whereas the visual and cerebellar networks had decreased FC. MoCA scores were adversely linked with decreased FC in the right parahippocampal gyrus (Han et al.,2020). According to Savoldi et al., patients with NMOSD had increased FC in the precuneus, right working memory network (WMN), several frontoparietal regions of the

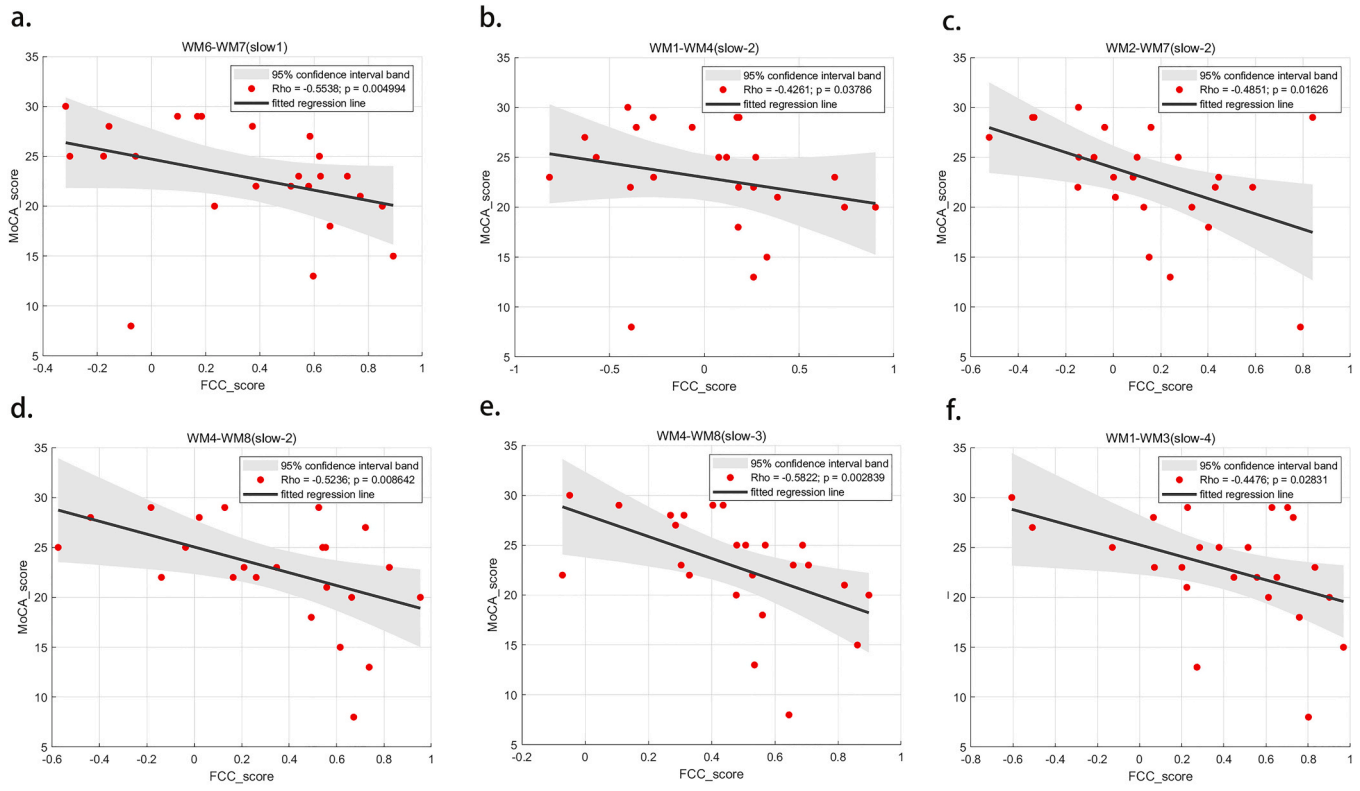

Fig. 6. A negative correlation between the MoCA scores and FCC in different bands. (a). WM6-WM7 (slow-1). (b). WM1-WM4 (slow-2). (c). WM2-WM7 (slow-2). (d). WM4-WM8 (slow-2). (e). WM4-WM8 (slow-3). (f). WM1-WM3 (slow-4).

salience network (SN), and both the bilateral and right WMN. In the left WMN, reduced frontal FC was detected in NMOSD (Savoldi et al.,2020). According to Yang et al., patients displayed decreased FC between the salience network (SN) and right frontoparietal network (rFPN) as well as between the SN and posterior DMN (Yang et al.,2022). Differences among the above studies may be attributed to sample heterogeneity, including the ethnic background, AQP4 antibody status, evaluation scale, definition and prevalence of CI, and applied research methodology.

To the best of our knowledge, these alterations in WM networks have been studied less. The WM of the human brain is a complex network, and a complete WM network is essential to maintaining human brain function. In the present study, multi-layer WM networks were revealed in patients with NMOSD (Table 2). WM networks consisted of three layers, including superficial (n = 5), middle (n = 2), and deep (n = 1) layers. The study examined the functional similarity between any two WM networks based on their connection patterns with GM regions. Compared with HCs, patients showed decreased FC in different layers of the WM networks (Fig. 2a), including WM1–4, WM1–8, WM2–6, WM2–7, WM2–8, WM4–8, WM5–8, which may be secondary to brain lesions or reduced local WM volume (Blanc et al.,2012, Finke et al., 2016).

As far as GM networks are concerned (Fig. 2b), the major networks, including GM1, GM2, GM3, GM4, GM5, GM6, and GM9, presented increased FC as well as decreased FC, while GM7 and GM8 showed decreased FC. Decreased FC may result in CI, whereas increased FC may indicate excessive information transmission or may be a compensatory mechanism. Interestingly, WM8 and WM6 were characterized by decreased FC in the WM and GM networks. The role of the local corpus callosum in cognitive function needs to be further studied by multimodal or radiomic MR studies. The patients showed decreased FC and FCC in WM networks, which were correlated negatively with the MoCA scores (Figs. 5, 6). Finally, different neural activities and physiological states may be reflected by different amplitudes in distinct frequency bands (Figs. 3, 4).

5. Limitations

The current study had several limitations. The number of patients in this study was low, which is explained by the low number of patients with NMOSD in a single medical center. Second, the MoCA scale is a screening tool for the assessment of patients' cognitive functions rather than a comprehensive cognitive test. Finally, AQP4 antibody-negative cases were not included.

6. Conclusions

In the present study, we first reported decreased spontaneous activity and reduced FC in WM networks, increased/decreased FC in GM networks, and a negative correlation between FC, FCC, and MoCA scores in WM networks. Our results provide a new method to understand the remodeling mechanism of cognitive function.

Funding

This work was supported by the Hainan Provincial National Science Foundation of China (822RC809), the National Science Foundation of China (U2033217, 62201133, 81360217), and the Project of Science and Technology Department of Hainan Province (ZDYF2021SHFZ095).

CRediT authorship contribution statement

Xincui Wan: Writing – original draft, Formal analysis. **Yingjie Tang:** Writing – original draft, Formal analysis. **Yu Wu:** Data curation. **Zhenming Xu:** Data curation. **Wangsheng Chen:** Supervision. **Feng Chen:** Supervision. **Cheng Luo:** Writing – review & editing, Methodology, Conceptualization. **Fei Wang:** Writing – review & editing, Methodology, Conceptualization.

Declaration of Competing Interest

The authors have no conflicts of interest to declare.

Data availability

Data will be made available on request.

Acknowledgements

We thank LetPub (www.letpub.com) for linguistic assistance.

References

Bigaut, K., Achard, S., Hemmert, C., et al., 2019. Resting-state functional MRI demonstrates brain network reorganization in neuromyelitis optica spectrum disorder (NMOSD). PLoS One 14, e0211465.
Blanc, F., Zéphir, H., Lebrun, C., et al., 2008. Cognitive functions in neuromyelitis optica. Arch. Neurol. 65, 84–88.
Blanc, F., Noblet, V., Jung, B., et al., 2012. White matter atrophy and cognitive dysfunctions in neuromyelitis optica. PLoS One 7, e33878.
Chanson, J.B., Zéphir, H., Collongues, N., et al., 2011. Evaluation of health-related quality of life, fatigue and depression in neuromyelitis optica. Eur. J. Neurol. 18, 836–841.
Cho, E.B., Han, C.E., Seo, S.W., et al., 2018. White matter network disruption and cognitive dysfunction in neuromyelitis optica spectrum disorder. Front Neurol. 9, 1104.
Cui, W., Shang, K., Qiu, B., et al., 2021. White matter network disorder in mesial temporal epilepsy, An fMRI study. Epilepsy Res 172, 106590.
Finke, C., Heine, J., Pache, F., et al., 2016. Normal volumes and microstructural integrity of deep gray matter structures in AQP4+ NMOSD. Neurol. Neuroimmunol. Neuroinflamm. 3, e229.
Han, Y., Liu, Y., Zeng, C., et al., 2020. Functional connectivity alterations in neuromyelitis optica spectrum disorder, correlation with disease duration and cognitive impairment. Clin. Neuroradiol. 30, 559–568.
He, D., Wu, Q., Chen, X., et al., 2011. Cognitive impairment and whole brain diffusion in patients with neuromyelitis optica after acute relapse. Brain Cogn. 77, 80–88.
Hollinger, K.R., Franke, C., Arenivas, A., et al., 2016. Cognition, mood, and purpose in life in neuromyelitis optica spectrum disorder. J. Neurol. Sci. 362, 85–90.
Hyun, J.W., Park, G., Kwak, K., et al., 2017. Deep gray matter atrophy in neuromyelitis optica spectrum disorder and multiple sclerosis. Eur. J. Neurol. 24, 437–445.
Jiang, Y., Song, L., Li, X., et al., 2019. Dysfunctional white-matter networks in medicated and unmedicated benign epilepsy with centrotemporal spikes. Hum. Brain Mapp. 40, 3113–3124.
Kawahara, Y., Ikeda, M., Deguchi, K., et al., 2014. Cognitive and affective assessments of multiple sclerosis (MS) and neuromyelitis optica (NMO) patients utilizing computerized touch panel-type screening tests. Intern Med 53, 2281–2290.
Kim, S.H., Kwak, K., Jeong, I.H., et al., 2016. Cognitive impairment differs between neuromyelitis optica spectrum disorder and multiple sclerosis. Mult. Scler. 22, 1850–1858.
Kim, S.H., Kwak, K., Hyun, J.W., et al., 2016. Widespread cortical thinning in patients with neuromyelitis optica spectrum disorder. Eur. J. Neurol. 23, 1165–1173.
Kim, S.H., Park, E.Y., Park, B., et al., 2017. Multimodal magnetic resonance imaging in relation to cognitive impairment in neuromyelitis optica spectrum disorder. Sci. Rep. 7, 9180.
Liu, Y., Liang, P., Duan, Y., et al., 2011. Abnormal baseline brain activity in patients with neuromyelitis optica, a resting-state fMRI study. Eur. J. Radio. 80, 407–411.
Liu, Y., Duan, Y., He, Y., et al., 2012. Altered topological organization of white matter structural networks in patients with neuromyelitis optica. PLoS One 7, e48846.
Liu, Y., Fu, Y., Schoonheim, M.M., et al., 2015. Structural MRI substrates of cognitive impairment in neuromyelitis optica. Neurology 85, 1491–1499.
Meng, H., Xu, J., Pan, C., et al., 2017. Cognitive dysfunction in adult patients with neuromyelitis optica: a systematic review and meta-analysis. J. Neurol. 264, 1549–1558.
Moore, P., Methley, A., Pollard, C., et al., 2016. Cognitive and psychiatric comorbidities in neuromyelitis optica. J. Neurol. Sci. 360, 4–9.
Peer, M., Nitzan, M., Bick, A.S., et al., 2017. Evidence for Functional Networks within the Human Brain's White Matter. J. Neurosci. 37, 6394–6407.
Power, J.D., Cohen, A.L., Nelson, S.M., et al., 2011. Functional Network Organization of the Human Brain. Neuron 72, 665–678.
Salama, S., Marouf, H., Reda, M.I., et al., 2020. Cognitive functions in Egyptian neuromyelitis optica spectrum disorder. Clin. Neurol. Neurosurg. 189, 105621.
Savoldi, F., Rocca, M.A., Valsasina, P., et al., 2020. Functional brain connectivity abnormalities and cognitive deficits in neuromyelitis optica spectrum disorder. Mult. Scler. 26, 795–805.
Shirer, W.R., Ryali, S., Rykhlevskaia, E., et al., 2012. Decoding Subject-Driven Cognitive States with Whole-Brain Connectivity Patterns. Cereb. Cortex 22, 158–165.
Vanotti, S., Cores, E.V., Eizaguirre, B., et al., 2013. Cognitive performance of neuromyelitis optica patients: comparison with multiple sclerosis. Arq. Neuropsiquiatr. 71, 357–361.
Wang, F., Liu, Y., Duan, Y., et al., 2011. Brain MRI abnormalities in neuromyelitis optica. Eur. J. Radio. 80, 445–449.
Wang, F., Liu, Y., Li, J., et al., 2017. Abnormal brain function in neuromyelitis optica, A fMRI investigation of mPASAT. Eur. J. Radio. 95, 197–201.
Wingerchuk, D.M., Banwell, B., Bennett, J.L., et al., 2015. International consensus diagnostic criteria for neuromyelitis optica spectrum disorders. Neurology 85, 177–189.
Yang, Y., Rui, Q., Wu, X., et al., 2022. Altered functional connectivity associated with cognitive impairment in neuromyelitis optica spectrum disorder. Mult. Scler. Relat. Disord. 68, 104113.
Zhang, N., Li, Y.J., Fu, Y., et al., 2015. Cognitive impairment in Chinese neuromyelitis optica. Mult. Scler. 21, 1839–1846.
Zheng, Q., Chen, X., Xie, M., et al., 2021. Altered structural networks in neuromyelitis optica spectrum disorder related with cognition impairment and clinical features. Mult. Scler. Relat. Disord. 48, 102714.